

---

## Turbulent Periodic Flow and Heat Transfer in A Square Channel with Different Ribs

Ahmed M. Bagabir<sup>1\*</sup>, Jabril A. Khamaj and Ahmed S. Hassan  
*Faculty of Engineering, Jazan University*  
*P. O. Box 706, Jazan, Saudi Arabia*

Received: 11/05/2013 – Revised 16/07/2013 – Accepted 19/07/2013

---

### Abstract

A numerical investigation has been carried out to examine turbulent flow and heat transfer characteristics in a three-dimensional ribbed square channels. Fluent 6.3 CFD code has been used. The governing equations are discretized by the second order upwind differencing scheme, decoupling with the SIMPLE (semi-implicit method for pressure linked equations) algorithm and are solved using a finite volume approach. The fluid flow and heat transfer characteristics are presented for the Reynolds numbers based on the channel hydraulic diameter ranging from  $10^4$  to  $4 \times 10^4$ . The effects of rib shape and orientation on heat transfer and pressure drop in the channel are investigated for six different rib configurations. Rib arrays of  $45^\circ$  inclined and  $45^\circ$  V-shaped are mounted in inline and staggered arrangements on the lower and upper walls of the channel. In addition, the performance of these ribs is also compared with the  $90^\circ$  transverse ribs.

*Keywords: Ribs; periodic flow; heat transfer; numerical simulation; turbulent.*

---

### 1. Introduction

Heat transfer enhancement is an active and important field of engineering research since it increases the effectiveness of heat exchangers. Suitable heat transfer augmentation techniques may achieve considerable technical advantages and savings of costs. There are various kinds of available techniques, adopted in many applications as gas turbine, heat exchanger, nuclear reactors, process industry and solar heater. The use of ribs mounted in the cooling or heating channels has been found to be an efficient technique of enhancing heat transfer by several investigators. The periodically positioned ribs in a channel interrupt hydrodynamic and thermal boundary layers. Ribs break the laminar sub-layer and create local wall turbulence due to flow separation and reattachment, which reduce thermal resistance and greatly augment the heat transfer. It is found that if ribs are placed at an inclination angle with respect to the axial direction, secondary flows are induced over the channel, resulting in the rise in the heat transfer rate towards the upstream region with respect to the downstream one [1, 2].

---

\* Corresponding Author: A. M. Bagabir  
Email: abagabir@yahoo.com Telephone: +966 546797778  
©2013 All rights reserved. ISSR Journals

Although heat transfer is increased through the use of ribs, the pressure drop of the channel flow is also increased due to the decreased flow area effects. Therefore, the shape, spacing, height and orientation of ribs are among the most important parameters used in the design of the channel of heat exchangers. Thus, it is difficult to realize the advantage of the rib geometry and arrangements.

Flow and heat transfer characteristics inside a ribbed channel depend on flow conditions and geometric configurations of the system. Many experimental and numerical investigations were carried out to determine configurations that produce optimum results in terms of both heat transfer and pressure loss. Previous studies show that there are many parameters involved in such studies:

- channel shape (e.g. [1]);
- channel aspect ratio,  $H/W$  (e.g. [1]);
- rib shape (e.g. [3- 6]);
- rib angle of attack, (e.g. [2-5]);
- rib width to rib height ratio,  $e/h$  (e.g. [7]);
- rib pitch to rib ratio,  $P/e$  (e.g. [7]);
- rib height to channel height ratio (blockage ratio),  $h/H$  (e.g. [1]);
- number of ribbed walls (e.g. [3]); and
- The manner by which ribs are positioned with respect to each other (inline/staggered) (e.g. [4]).

It is found that the increase in rib width has an adverse effect on the heat transfer performance. The square rib produced the best heat transfer performance [7]. From the hydrodynamic point of view, since the pressure drop is raised as the rib height increases, the optimum blockage ratio,  $h/H$ , is known to be around 0.1 [8, 9]. The pitch also has an optimum, because it should be longer than the recirculation zone formed behind the rib. The recommended ratio of the rib pitch to height is about 10 for the Reynolds number range of interest [8, 9]. Flow parameters such as the Reynolds number is also of critical importance. The Reynolds number,  $Re$ , based on the bulk velocity and hydraulic diameter, ranges from  $10^4$  to  $10^5$  in the internal cooling channel of turbine blade.

On the other hand, many studies have been conducted to examine thermal and flow characteristics for using ribs to promote heat transfer in the channel walls. An experimental study of Han *et al.* [3], on heat transfer behaviors in a square channel with different inline inclined ribs, showed that the inclined and V-shaped ribs provides higher heat transfer enhancement than transverse rib. For heating either one of the ribbed walls only or both of them, or all four channel walls, they [3] reported that the former two conditions resulted in an increase in the heat transfer with respect to the latter one. Khamaj [1] experimentally investigated the internal cooling channel of a turbine blade. He developed heat transfer correlations for turbulence air flow in static and rotating rectangular channels with  $45^\circ$  inclined ribs on two opposite wall. A numerical investigation of Murata and Mochizuki [10] on heat transfer characteristics in a ribbed square channel with  $60^\circ$  orientation showed that the flow reattachment caused a significant increase in the local heat transfer. Patankar *et al.* [11] introduced the concept of periodically fully developed flow to investigate numerically the flow and heat transfer characteristics in a channel and since then, periodic channel flows have been applied extensively.

The present work extends the experimental investigation of internal cooling channel of a turbine blade carried out in the previous study of Khamaj [1]. The aim of the present analysis is to investigate the flow and the heat transfer characteristics of a rib-roughened square channel with the upper and bottom walls subjected to uniform heat flux by means of Fluent 6.3 code [12]. The numerical simulations have been applied to help in the interpretation and to gain a more solid understanding of these complicated flow fields and to achieve a better

understanding of the ongoing processes. The objective of this study is to compare the heat transfer characteristics, the friction losses and the thermal performance for different rib shapes and orientations for both inline and staggered arrangements with varying Reynolds numbers in the range between  $10^4$  and  $4 \times 10^4$ . The numerical computations are performed for three-dimensional turbulent periodic channel flows over  $90^\circ$ ,  $45^\circ$  inclined and  $45^\circ$  V-shaped ribs mounted periodically.

## 2. Flow configuration

The flow is computed in a square cross-sectioned channel with a  $45^\circ$  inclined and  $45^\circ$  V-shape ribs. This geometry is representative of a high pressure turbine blade cooling channel. The ribs are placed on the upper and lower channel walls for both inline and staggered arrangements as shown in Fig. 1. Ribs are provided on the heated walls. For rib pairs arranged in staggered manner, the upper surface is moved to the right by half the inter-rib spacing (see Fig. 1). The computational domain and the grid size for both inline and staggered configurations are similar. The flow under consideration is expected to attain a periodic flow condition in which the velocity field repeats itself [11]. As a result, the simulation is limited to a single pitch. The upstream and downstream boundaries have the same inclination angle as the rib (see Fig. 1). The air enters the channel at an inlet temperature and flows over square rib of length,  $h = e = 2.5 \text{ mm}$ . The channel height,  $H$ , is set to  $0.014 \text{ m}$ , and the pitch,  $p$ , or distance between ribs is set to  $0.02 \text{ m}$ . The pitch to rib ratio ( $P/e$ ) is 8 and the ratio between rib height and hydraulic diameter of the channel ( $h/D$ ) is 0.1786. Also, a typical transverse rib ( $\alpha = 90^\circ$ ) is introduced for comparison.

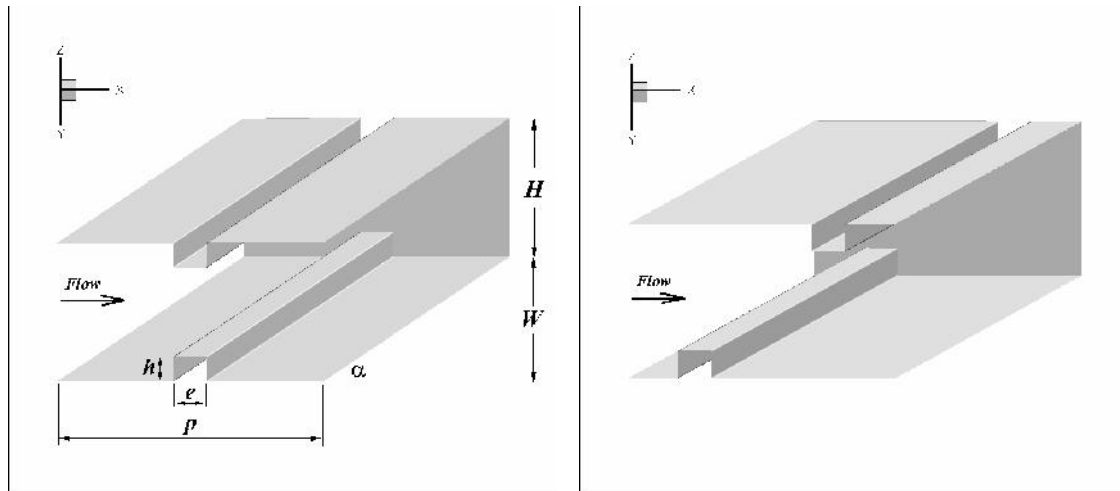


Figure 1. Computational domains of periodic flow for inline (left) and staggered (right) ribs.

Periodic boundaries are used for the inlet and outlet of the flow domain. The inlet and outlet profiles for the velocities must be identical. Constant mass flow rate of air is assumed in the flow direction due to the periodic flow conditions. Also a mean bulk temperature of  $300\text{K}$  is applied at the inlet. The physical properties of the air were assumed to remain constant at average bulk temperature. Impermeable boundary and no-slip wall conditions were implemented over the channel walls as well as the ribs. The two opposite walls with the ribs are assumed heated surfaces with constant heat flux of  $17577 \text{ W/m}^2$ , while the other two walls are kept adiabatic. The ribs are assumed at conjugate wall (low thermal resistance) conditions. To simplify the calculations, a symmetry condition is applied. The computational domain is resolved by regular Cartesian elements. The grids are refined near the wall surfaces using grid

adaption technique employed by Fluent 6.3 which refines the grid based on geometric and numerical solution data [12]. Considering both convergent time and solution precision, the grids shown in Table 1 are adopted for the current computational models using similar grid density.

TABLE 1: GRID DETAILS FOR DIFFERENT CASES

Case	No. of cells	Symmetry plane(s)
Inline 90°	39315	xy and xz planes
Inline 45°	104840	xz plane
Inline 45° V	52420	xy and xz planes
Staggered 90°	78630	xy plane
Staggered 45°	209680	-
Staggered 45° V	104840	xy plane

### 3. Mathematical modelling

The numerical model for fluid flow and heat transfer in a channel is developed under the following assumptions:

- Steady three-dimensional fluid flow and heat transfer.
- Periodic, fully developed, turbulent and incompressible flow.
- Constant fluid properties.
- Ignored body forces.
- Negligible radiation heat transfer.

Subsequently, the channel flow is governed by the continuity, the Reynolds averaged Navier–Stokes (RANS) equations and the energy equation. In the Cartesian tensor system these equations can be written as follows:

Continuity equation:

$$\frac{\partial}{\partial x_i} (\dots u_i) = 0 \quad (1)$$

Momentum equation:

$$\frac{\partial}{\partial x_j} (\dots u_i u_j) = \frac{\partial p}{\partial x_i} + \frac{\partial}{\partial x_j} \left[ \sim \left( \frac{\partial u_i}{\partial x_j} - \dots \overline{u'_i u'_j} \right) \right] \quad (2)$$

where ... is the density of fluid, and  $u_i$  is the mean component of velocity in  $x_i$  direction,  $p$  is the pressure,  $\mu$  is the dynamic viscosity, and  $u'$  is a fluctuating component of velocity. Repeated indices indicate summation from one to three for three-dimensional problems. The Reynolds-averaged approach of turbulence modelling utilizes the Boussinesq hypothesis to relate the Reynolds stresses in the above equation to the mean velocity gradients as:

$$- \dots \overline{u'_i u'_j} = \sim_t \left( \frac{\partial u_i}{\partial x_j} + \frac{\partial u_j}{\partial x_i} \right) - \frac{2}{3} \left( \dots k + \sim_t \frac{\partial u_i}{\partial x_i} \right) \delta_{ij} \quad (3)$$

where  $k$  is the turbulent kinetic energy defined by  $k = \dots \overline{u'_i u'_i}$ , and  $\delta_{ij}$  is the *Kronecker* delta.

Energy equation:

$$\frac{\partial}{\partial x_i} (\dots u_i T) = \frac{\partial}{\partial x_j} \left[ (X + X_t) \frac{\partial T}{\partial x_j} \right] \quad (4)$$

where  $X$  and  $X_t$  are molecular thermal diffusivity and turbulent thermal diffusivity, respectively and are given by  $X = \sim / Pr$ ,  $X_t = \sim_t / Pr_t$ .

The selection of the suitable turbulence model is very important in any computational analysis to predict the accurate results. The analysis consists of flow with low Reynolds number. The standard  $k$ - $\tilde{S}$  and realizable  $k$ - $\nu$  turbulence model are generally used for low Reynolds number analysis. However, three turbulence models are investigated namely the renormalization group (RNG)  $k$ - $\nu$  [13], realizable  $k$ - $\nu$  [14] and shear-stress transport (SST)  $k$ - $\tilde{S}$  [15]. The  $k$ - $\nu$  turbulence models are incorporated with a well-established non-equilibrium wall function for the near wall treatment. The equations governing the turbulence models will not be given here. Readers who are interested in these models are advised to refer to the above mentioned studies.

The commercial Fluent 6.3 CFD code has been used in this work [12]. The governing equations are discretized by the second order upwind differencing scheme, decoupling with the SIMPLE algorithm and are solved using a finite volume approach. The energy equations are solved after the flow and turbulence equations in a segregated fashion. The  $y^+$  value of the near-wall nodes is kept, in all computations, to less than 10. The solutions are considered to be converged when the normalized residual values are less than  $10^{-6}$  for all variables but less than  $10^{-8}$  only for the energy equation. Four parameters of interest in the present work are the Reynolds number, Nusselt number, friction factor and thermal enhancement factor. The Reynolds number,  $Re$ , is based on the bulk velocity,  $U_m$ , and hydraulic diameter,  $D$ . The thermal performance is measured by the heat transfer coefficient,  $h$ , and Nusselt number,  $Nu$ , which can be written as:

$$h = \frac{q}{T_S - T_B} ; \quad Nu = hD/k \quad (5)$$

Where,  $T_B$  is the bulk temperature of fluid over the cross section,  $T_S$  is the channel wall temperature,  $q$  is the heat flux and  $k$  is the thermal conductivity. The  $Nu$  is normalized by Nusselt number for a smooth channel,  $Nu_0$ , which is given by Dittus–Boelter formula operated at the same Reynolds number:

$$Nu_0 = 0.023 Re^{0.8} Pr^{0.4} \quad (6)$$

The friction factor,  $f$ , is computed by pressure drop,  $Up$ , across the length of the periodic channel,  $l$  (=rib pitch spacing) as:

$$f = \frac{(Up/l)D}{0.5 \dots u_m^2} \quad (7)$$

The relative importance of the pumping power can be assessed by comparing the friction factor with the one associated with the flow in a smooth pipe,  $f_0$ , which is given by the Blasius correlation:

$$f_0 = 0.046 Re^{-0.2} \quad (8)$$

The thermal enhancement factor,  $TEF$ , is defined as the ratio of the heat transfer coefficient of an augmented surface to that of a smooth surface at an equal pumping power. It is given by:

$$TEF = (Nu/Nu_0) / (f/f_0)^{1/3} \quad (9)$$

## 4. Results and discussion

### 4.1. Code validation

The present numerical method is validated by comparing its results with the corresponding experimental data of Khamaj [1] for the average Nusselt numbers at wall surface. The calculations are performed in a double wall ribbed square channel with inline  $45^\circ$  inclined rib arrays. The computed average Nusselt numbers using different turbulence models are shown in Fig. 2. The percentage error is very high for realizable  $k$ - $\nu$  (RKE) model which is about 20%. The percentage error is 12% for SST  $k$ -

$\tilde{S}$  turbulence model. It is clear that the RNG  $k$ - $\nu$  model exhibits best results and predicts the overall heat transfer rate in excellent agreement with the experimental results of Khamaj [1]. It shows less than 6% deviation from experimental results. The difference in the averaged heat transfer predictions is related to the large scale motion of the flow field (e.g. reattachment lengths) which is not properly reflected in the realizable  $k$ - $\nu$  and SST  $k$ - $\tilde{S}$  models. Although the RNG  $k$ - $\nu$  turbulence model reveals the best accuracy of heat transfer, the other turbulence models ensure better convergence performance and less computational time. However, the agreement found between the measured value and the numerical computations using RNG  $k$ - $\nu$  model is rather encouraging. Therefore, the RNG  $k$ - $\nu$  model is used for the rest of the calculations in the present study. On the other hand, the standard  $k$ - $\tilde{S}$  model is also investigated. Its outcome displays a solution almost identical to the SST model. This is expected because the SST  $k$ - $\tilde{S}$  model incorporates a blending function that allows it to switch from the standard  $k$ - $\tilde{S}$  model in the near-wall region to a high Reynolds number version of the  $k$ - $\tilde{S}$  model in the free stream. Therefore, it is omitted from the comparisons.

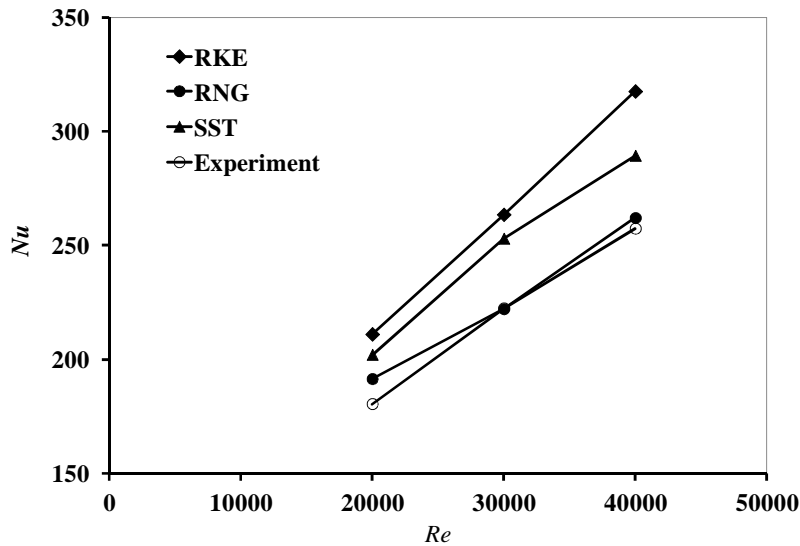


Figure 2. Average Nusselt number for different turbulence models compared with the experimental results of Khamaj [1] at different Reynolds numbers.

#### 4.2. Flow structure

It is necessary to understand the flow structure and behaviour in the ribbed channel before discussing the results. The flow structure in the channel mounted periodically with various ribs can be displayed by considering the streamtraces as depicted in Fig. 3 for  $90^\circ$  transverse,  $45^\circ$  inclined and inline  $45^\circ$  V-shaped ribs, respectively. The streamtraces are presented at Reynolds number of  $Re=3 \times 10^4$ . As shown in Fig. 3, the flow field is dominating by large-scale and small-scale vortex structures. The large-scale coherent structure initiates at upstream and presents above the upstream and on the downstream part of the rib. The large vortex which arches through the channel is twice the length of the pitch and has a major influence on the flow.

For the transverse rib, the large vortex appears at side walls and small structure on the downstream is also visible on the figure. Only two transverse vortices moved

towards the side walls are found and trapped behind each rib. Moreover, for 90° rib, the flow moves upwards by the secondary flow near side walls. The presence of inclined and V-shaped ribs creates two main counter rotating vortices resulting in longer flow path and high strength of vortex due to changing in its orientation (see Fig. 3). The most notable characteristics of the effects of the inclined and V-shaped ribs on the mainstream flow are flow separation, recirculation, and inclined secondary flow (see Fig. 3). As the mainstream flow passes over the 45° and 45° V-shaped ribs, it separates and creates vortex flow behind the rib due to high pressure difference across the rib before moving helically along the rib downstream, then rolling up. Also the mixing of the streamtraces initialized from various positions can be followed clearly in the cases of inclined and V-shaped ribs. This flow mixing between the main and the wall regions leads to relatively high heat transfer.

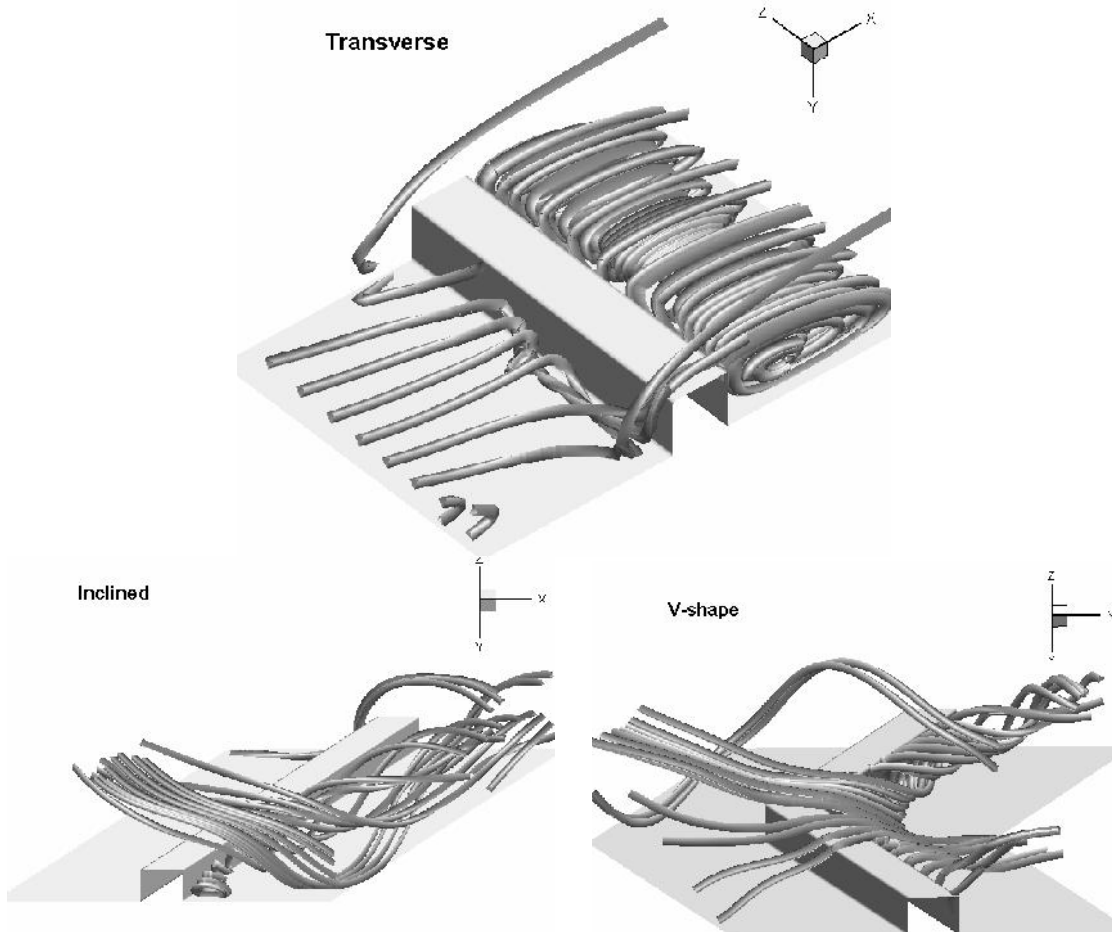


Figure 3. Streamtraces for transverse, inclined, and V-shaped rib arrays arranged in the inline configuration at  $Re=3 \times 10^4$ .

#### 4.3. Heat transfer

Figure 4 displays contour maps of normalized temperature,  $T/T_{in}$ , for 90°, 45° and 45° V-shaped ribs arranged in the inline and staggered arrays at Reynolds number of  $Re=3 \times 10^4$ . Similar contour levels and numbers are applied. The contour maps show that there is a major change in the temperature field over the ribbed channels.

The contour map of normalized temperature field for the  $90^\circ$  ribs shows that the higher temperature gradient can be observed almost in the downstream and over the rib where the lower one can be found in the upstream region (see Fig. 4). The major change in the temperature field is found in the upstream and over the rib, while in the downstream, there is a minor change. The contour maps and the average normalized temperature values, shown in a bracket above the contour legend, reveal that the inline and staggered orientations of the transverse rib generate almost similar results (see Fig. 4). For the fully developed flow, hot spots exist in the recirculation region immediately downstream the square  $90^\circ$  ribs because the fluid flow is nearly stagnant relative to the mainstream in this region (see Fig. 4). The hot spots lead to lower heat transfer coefficient from the surface. This implies that the transverse recirculation zone upstream of the rib provides a significant influence on the temperature field while the flow in the rib downstream is not affected by the presence of the  $90^\circ$  rib. Therefore, it is of interest to know whether the channel roughened with ribs of different shape can improve the heat transfer rate.

It appears that, in comparison with the  $90^\circ$  case, the lower temperature values over the heated surface with the inclined and V-shaped ribs are seen in a larger area, except for small regions near the sidewalls (see Fig. 4). This indicates the merit of employing such ribs over a smooth channel for enhancing heat transfer. For inclined and V-shaped rib cases, the vortex flows provide a significant influence on the temperature field, because it can induce better fluid mixing between the wall and the main flow. The higher temperature gradient can be observed where the flow impinges the side channel wall. It is obvious that the  $45^\circ$  V-shaped ribs orientation enhances the heat transfer better than  $45^\circ$  inclined ribs. For the V-shaped rib, two pair of large-scale counter-rotating secondary flow is induced in the channel [3]. For the V-shaped rib configurations, the temperature maps show the minimum values at the centre region, and increases gradually along the ribs towards sidewalls due to the two pairs of counter-rotating secondary flows generated in the channel. Moreover, the temperature maps and the average normalized temperature values of V-shaped ribs illustrate that when the ribs are arranged in the inline orientation, they produce better rate of heat transfer than staggered ribs (see Fig. 4). This is could be attributed to the stronger counter-rotating secondary flows in the case of the inline rib configuration which reduces the size of the developed boundary layer.

On the other hand, the local variation of the normalized Nusselt number,  $Nu/Nu_0$ , in the streamwise direction at three spanwise locations (centreline and side walls) in between the ribs, is shown in Fig. 5. The considered cases are  $90^\circ$ ,  $45^\circ$  and  $45^\circ$  V-shaped ribs arranged in the inline configuration at Reynolds number of  $Re=3\times 10^4$ . Heat transfer enhancements along the streamwise direction are attributed to the flow separation and reattachment. The presence of ribs locally reduces the channel area resulting in the acceleration of the flow around the ribs. The acceleration and sudden expansion of this flow separates it which again reattaches further downstream. The  $90^\circ$  case shows the highest  $Nu/Nu_0$  values at the sidewalls and the lowest at the centre region. Although, the  $45^\circ$  V-shaped rib reveals the highest Nusselt number values at the centre region, it shows big variations between the upstream and downstream sides of the rib. Moreover, the plots of Fig. 5 indicate that the heat transfer is reduced downstream of the rib near back wall of  $45^\circ$  case and near the sidewalls of the  $45^\circ$  V-shaped rib. The heat transfer in these zones is even lower than the heat transfer of a smooth channel with no rib. However, when compared with the  $45^\circ$  layout, the  $45^\circ$  V-shaped rib shows improvement of heat transfer at the upstream of the rib.

When the solutions are averaged over appropriate areas, they provide engineering information about the heat transfer and friction. The variation of the average normalized Nusselt number,  $Nu/Nu_0$ , with the Reynolds number for ribs of various shapes and arrangements is depicted in Fig. 6. In general, as the Reynolds number increases, the average Nusselt number,  $Nu$ , for a channel increases. This is due to the increase in velocity which causes turbulence. Since the rate of increase in Nusselt number is low, the  $Nu/Nu_0$  values have a negative slope as the Reynolds number increases. Therefore, as shown in Fig. 6, the average normalized Nusselt number,  $Nu/Nu_0$ , decreases as the Reynolds number increases.

For the considered cases, the analysis of Fig. 6 reveals that the introducing of ribs yields heat transfer rate about 2.3–5.8 times higher than the smooth channel with no rib. Thus, the generation of vortex flows from using rib as well as the role of better fluid mixing and the impingement are the reason for the augmentation of heat transfer in a ribbed channel. The  $45^\circ$  and  $45^\circ$  V-shaped ribs perform much better than the  $90^\circ$  rib for enhancing heat transfer. Moreover, the Nusselt number values for both the  $45^\circ$  and  $45^\circ$  V-shaped ribs are found to be about 17%–50% over that for the rib placed transversely to the main stream direction. On the other hand, the inline and staggered rib orientations of  $90^\circ$  and  $45^\circ$  cases reveal identical heat transfer performance for all considered Reynolds number. However, for the  $45^\circ$  V-shaped ribs, it is noted that the inline performs 15% better than the staggered arrangement. The inline and staggered inclined ribs perform nearly the same heat transfer rate as the staggered V-shaped ribs at Reynolds number greater than  $2 \times 10^4$  (see Fig. 6). It is clear that the inline  $45^\circ$  V-shaped rib represents the best rib shape and orientation for heat transfer augmentation. This indicates that this case produces strong vortex which yields a mixing intensity of the flow.

#### 4.4. Pressure loss

In general, the heat transfer augmentation is concerned with penalty in terms of increased friction coefficient resulting in higher pressure drop. It is found that the friction factor follows a different pattern from Nusselt number. The average normalized friction factor,  $f/f_0$ , increases as the Reynolds number increases for various rib shapes and orientations as depicted in Fig. 7. It is obvious that all considered ribs create friction factor higher than smooth channel with no rib. Figure 7 illustrates that the staggered orientation generates lower friction factor for  $90^\circ$  and  $45^\circ$  V-shaped ribs than their inline arrangement. The staggered  $90^\circ$  rib offers the lowest flow resistance among all configurations. In contrast, it reveals friction factor of about 150% lower than its corresponding inline orientation.

For the  $45^\circ$  V-shaped rib, the staggered configuration provides about 10% lower friction factor than the inline one. On the other hand, as depicted Fig. 7, it is found that the inline configuration is preferable for the  $45^\circ$  rib.

#### 4.5. Performance evaluation

Figure 8 exhibits variation of the thermal enhancement factor,  $TEF$ , for air flowing in square channels of two ribbed walls. As depicted in the figure, the thermal enhancement factor tends to decrease with the rise of the Reynolds number. Meanwhile, it shows an increase trend for the inline  $45^\circ$  V-shaped rib for the Reynolds number greater than  $3 \times 10^4$ . The enhancement factors of the ribs considered in this study are seen to be above unity. They vary between 1.3 and 4.2 per unit pumping power, depending on the Reynolds number. This indicates that these cases are

advantageous with respect to smooth channel with no rib. It is found that the inline 90° rib yield the lowest thermal enhancement factor. This is the reason why it is not used a lot to enhance heat transfer in many thermal engineering applications in comparison with other orientations. It seems that the inline configuration is preferable for the inclined and V-shaped ribs especially at low Reynolds number of  $Re=10^4$ . At Reynolds number of  $Re=10^4$ , the inline 45° rib is found to have the highest channel heat transfer per unit pumping power.

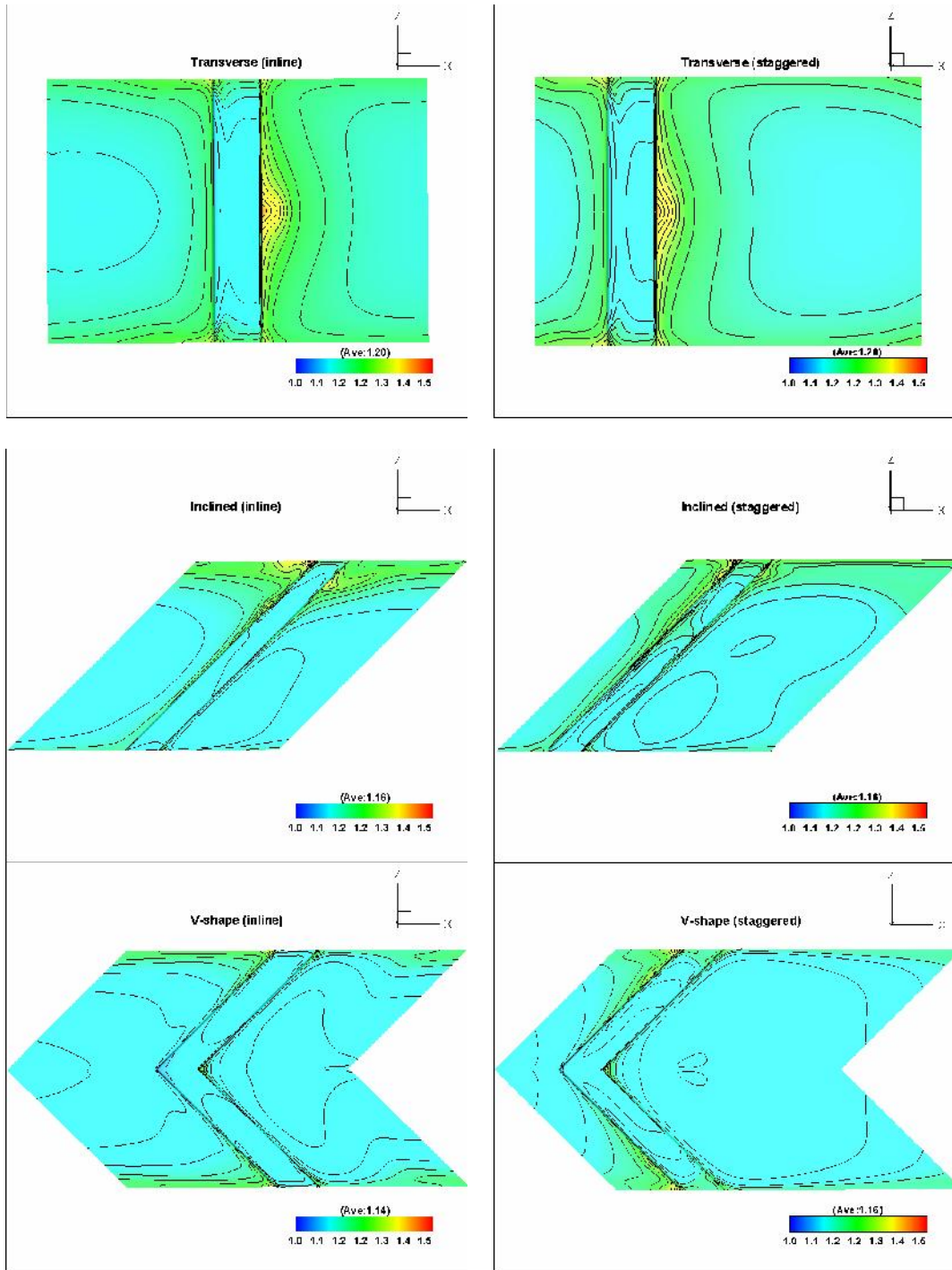


Figure 4. Normalised temperature ( $T/T_{in}$ ) maps for different ribs at  $Re=3 \times 10^4$ .

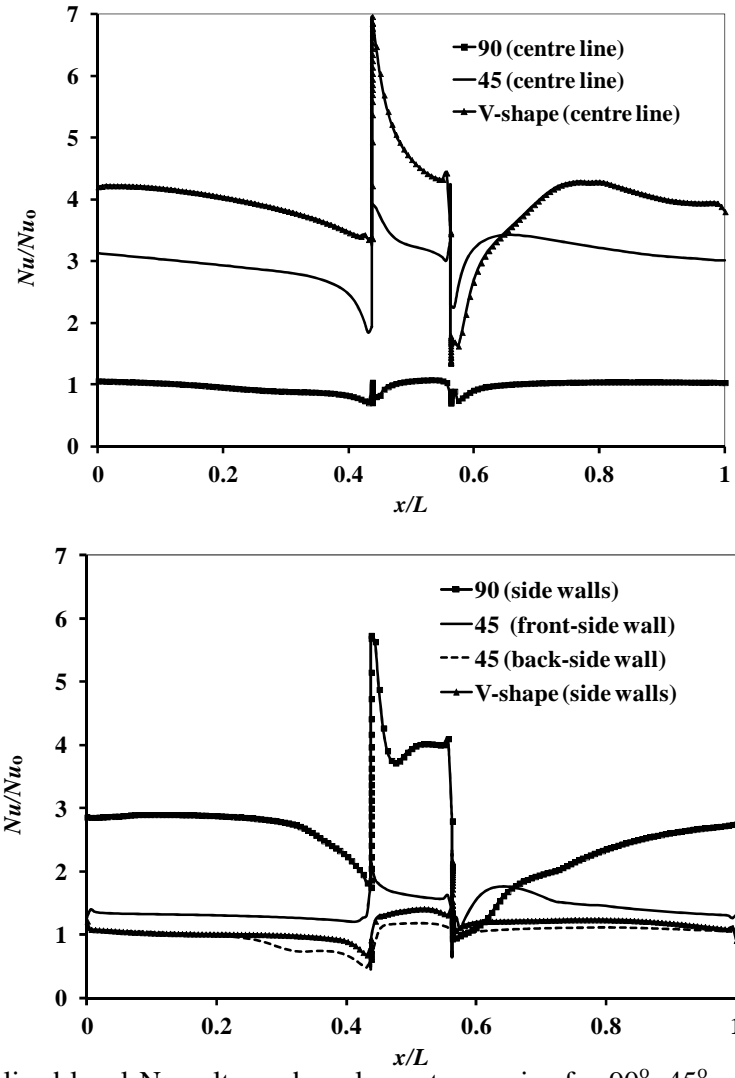


Figure 5. Normalised local Nusselt number along streamwise for 90°, 45° and 45° V-shaped ribs arranged in the inline configuration at  $Re=3 \times 10^4$ .

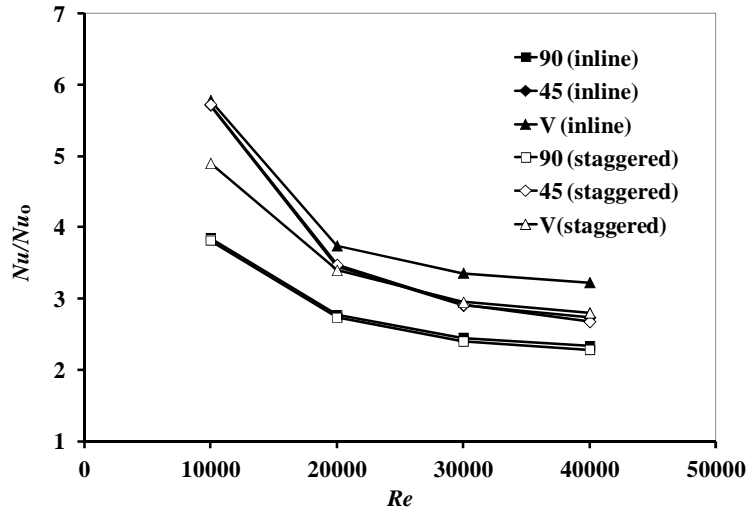


Figure 6. Variation of average normalized Nusselt number,  $Nu/Nu_0$ , with Reynolds number for different ribs.

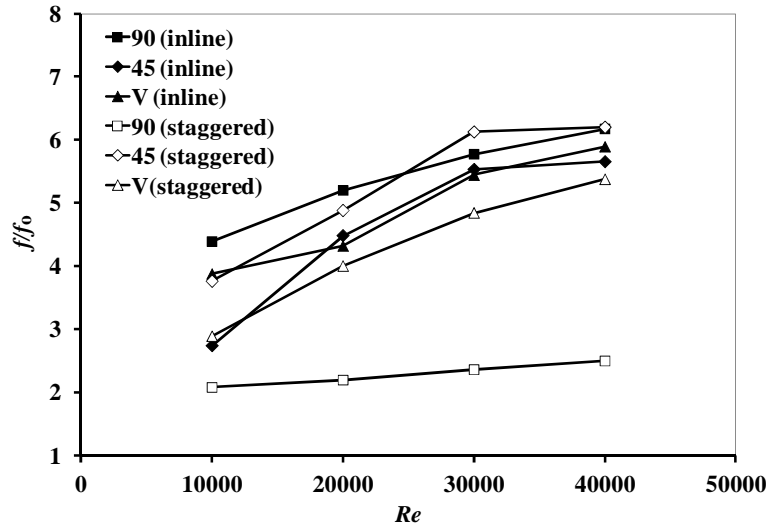


Figure 7. Variation of average friction factor,  $f/f_0$ , with Reynolds number for different ribs.

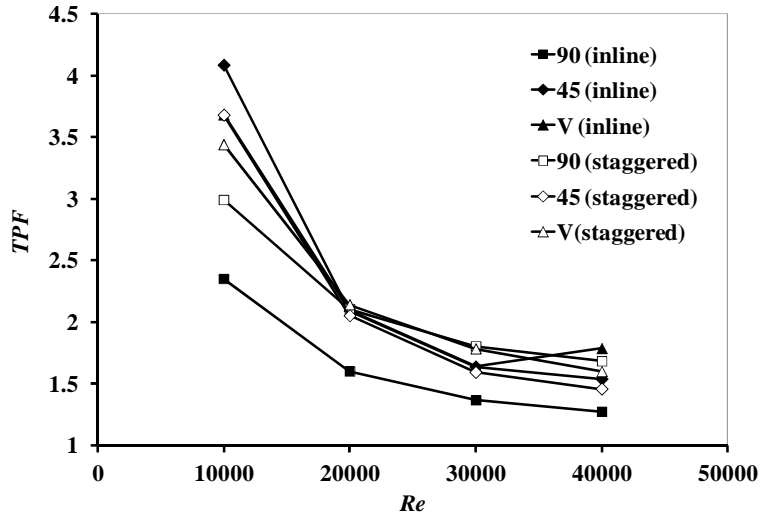


Figure 8. Variation of thermal enhancement factor,  $TEF$ , with Reynolds number for different ribs.

## 5. Conclusions

Turbulent periodic flow and heat transfer characteristics in a square channel fitted with  $45^\circ$  inclined and  $45^\circ$  V-shaped ribs in tandem have been investigated numerically. The rib arrays are set in inline and staggered arrangements on two opposite walls. The vortex flows created by using such ribs help to induce strong rotational momentum of the secondary flows leading to drastic increase in heat transfer in the square channel compared with  $90^\circ$  transverse ribs. However, the temperatures maps demonstrate that the  $45^\circ$  V-shaped rib improve the heat transfer rate better than  $45^\circ$  inclined rib especially near side walls. It is apparent that the main flow induces two impinging flows on each sidewall of V-shaped rib leading to an increase in heat transfer rate over the channel.

In general, the order of heat transfer enhancement in the channel with two ribbed walls is about 230–580% higher than the smooth channel with no rib. However, the heat transfer

augmentation is associated with enlarged friction loss ranging from 2.0 to 6.2 times above the smooth channel. Moreover, the inclined and V-shaped rib pairs arranged in the inline manner reveal heat transfer improvement of about 17-50% higher than that for the 90° rib; whereas the pressure loss can be reduced at about 4-38% depending on Reynolds number. It is found that the staggered inclined ribs produces similar thermal profile as inline orientation but with higher friction factor. The staggered orientation lowers the thermal performance of 45° V-shape and reduces the friction factor. On the contrary, the staggered 90° transverse rib reveals thermal enhancement factor similar to inclined and V-shaped ribs for Reynolds number equal or higher than  $2 \times 10^4$ . For Reynolds number of  $10^4$ , the inline 45° rib reveals the optimum thermal enhancement factor.

## References

- [1] Khamaj, J., *An experimental study of heat transfer in the cooling channels of gas turbine rotor blades*. PhD Thesis, University Wales, UK (2002).
- [2] Manca O., Nardini S. and Ricci D. *Numerical study of air forced convection in a channel provided with inclined ribs*. *Frontiers in Heat and Mass Transfer*, 2011. **2**. DOI: [10.5098/hmt.v2.1.3007](https://doi.org/10.5098/hmt.v2.1.3007).
- [3] Han J.C., Zhang Y.M., Lee C.P. *Augmented heat transfer in square channels with parallel, crossed and V-shaped angled ribs*. ASME, *Journal of Heat Transfer* 1991. **113**: 590–596.
- [5] Liu H. and Wang J. *Numerical investigation on synthetical performances of fluid flow and heat transfer of semiattached rib-channels*. *International Journal of Heat and Mass Transfer*, 2011. **54**: 575–583.
- [6] Promvong P., Changcharoen W., Kwankaomeng S. and Thianpong C. *Numerical heat transfer study of turbulent square-duct flow through inline V-shaped discrete ribs*. *International Communications in Heat and Mass Transfer*, 2011. **38**: 1392–1399.
- [7] Kamali R. and Binesh A.R. *The importance of rib shape effects on the local heat transfer and flow friction characteristics of square ducts with ribbed internal surfaces*. *International Communications in Heat and Mass Transfer*, 2008. **35**: 1032–1040.
- [8] Sampath A. R. *Effect of rib turbulators on heat transfer performance in stationary ribbed channels*, PhD Thesis, Cleveland State University, USA (2009).
- [9] Han J.C. *Heat transfer and friction in channels with two opposite rib roughened walls*. ASME J. Heat Transfer, 1984. **106**: 774–781.
- [10] Liou T.-M. and Hwang J.-J. *Turbulent heat transfer and friction in periodically fully developed channel flows*. ASME J. Heat Transfer, 1992. **114**: 56–64.
- [11] Murata A. and Mochizuki S. *Comparison between laminar and turbulent heat transfer in a stationary square duct with transverse or angled rib turbulators*. *International Journal of Heat and Mass Transfer*, 2001. **44**: 1127–1141.
- [12] Patankar S.V. Liu C.H. and Sparrow E.M. *fully developed flow and heat transfer in ducts having streamwise-periodic variations of cross-sectional area*. ASME Journal of Heat Transfer, 1977. **99**: 180–186.
- [13] Fluent Corporation, *Fluent v6.3 user guide* (2006).
- [14] Yakhot V. and Orszag S. A. *Renormalization Group Analysis of Turbulence: I. Basic Theory*. *Journal of Scientific Computing*, 1986. **1**(1):1–51.
- [15] Shih T.-H., Liou W. W., Shabbir A., Yang Z., and Zhu J. *A New k- $\nu$  Eddy-Viscosity Model for High Reynolds Number Turbulent Flows- Model Development and Validation*. *Computers Fluids*, 1995. **24**(3):227–238.
- [16] Menter F. R. *Two-Equation Eddy-Viscosity Turbulence Models for Engineering Applications*. *AIAA Journal*, 1994. **32**(8):1598–1605.

## Nomenclature

---

$D$	Hydraulic diameter of channel width ( $m$ )
$e$	Rib width ( $m$ )
$f$	Friction factor for a ribbed channel
$f_0$	Friction factor for a smooth channel
$h$	Rib height ( $m$ ), heat transfer coefficient ( $W/m^2K$ )
$H$	Channel height ( $m$ )
$k$	Thermal conductivity ( $W/mK$ ) or turbulent kinetic energy ( $kJ/kg$ )
$Nu$	Nusselt number of a ribbed channel
$Nu_0$	Nusselt number of a smooth channel
$p$	static pressure ( $pa$ ) or rib pitch spacing ( $m$ )
$Pr$	Prandtl number,
$q$	Heat flux ( $W/m^2$ )
$Re$	Reynolds number
$T_B$	Bulk temperature of flow ( $K$ )
$T_S$	Surface temperature ( $K$ )
$T_w$	Wall temperature ( $K$ )
$TEF$	Thermal enhancement factor
$u$	Velocity ( $m/s$ )
$U_m$	Bulk velocity ( $m/s$ )
$W$	Channel width ( $m$ )
...	Density ( $kg/m^3$ )

---